Available online at www.sciencedirect.com
ScienceDirect
Ceramics International 34 (2008) 1643–1651
CERAMICS INTERNATIONAL
www.elsevier.com/locate/ceramint

Carbothermal reduction–nitridation of titania-bearing blast furnace slag

Tao Jiang *, Xiangxin Xue, Peining Duan, Xin Liu, Shuhui Zhang, Ran Liu

School of Materials and Metallurgy, Northeastern University, Shenyang 110004, PR China

Received 6 July 2006; received in revised form 26 March 2007; accepted 12 July 2007
Available online 10 August 2007

Abstract

The synthesis of (Ca,Mg)α′-Sialon ($(Ca,Mg)_xSi_{12-3x}Al_{3x}O_xN_{16-x}$) powders using titania-bearing blast furnace slag as a starting material by carbothermal reduction–nitridation (CRN) was reported for the first time. The reaction processes were greatly affected by initial material and reaction parameters. With the compositions shifting range from $x = 0.3$ up to 2.0, the amount of (Ca,Mg)α′-Sialon, TiN and AlN, the solid solubility of Ca^{2+} and Mg^{2+}, the unit cell parameters of the (Ca,Mg)α′-Sialon and the amount of elongated α′-Sialon grains increased, but β′-Sialon and SiC decreased. With the increase of synthesis temperature and holding time, the formation of (Ca,Mg)α′-Sialon in the products increased and the CRN reactions accelerated. The optimum synthesis conditions of (Ca,Mg)α′-Sialon were 1480 °C for 8 h, under which the crystalline phases of the products also included AlN, TiN and a small amount of SiC and β-$CaSiO_3$. The volatilization of SiO resulted in a mass loss of samples, which was enhanced with the increase of synthesis temperature and holding time.

Keywords: (Ca,Mg)α′-Sialon; Carbothermal reduction–nitridation; Titania-bearing blast furnace slag; Powder synthesis

1. Introduction

Recycling of industrial wastes is gaining more and more attention owing to the ever-increasing worldwide consciousness about environmental protection. Blast furnace slag is a waste product from metallurgical plants and is produced on a daily basis in large quantities. For example, the annual slag production for the PanSteel Company in Sichuan is about 3.0×10^6 tonnes. Therefore, there are both economical and ecological reasons to try to reuse the wasteful slag. Titania-bearing blast furnace slag mainly contains CaO, SiO_2, Al_2O_3, MgO and TiO_2, which are raw materials for synthesizing (Ca,Mg)α′-Sialon by carbothermal reduction–nitridation (CRN). In this process TiO_2 convert into TiN phase that possess high-melting point, high hardness and high-electrical conductivity, which can improve the combination properties of materials. α′-Sialon is represented by a general formula $M_x{}^{v+}Si_{12-(m+n)}Al_{(m+n)}O_nN_{16-n}$ (M represents Li, Ca, Mg, Y and most of lanthanide elements. $x = m/v$, v is the valency of the cation). Substitution of m(Al–N) and n(Al–O) bonds for $(m + n)$(Si–N) bonds occurs in the α′ structure. The charge imbalance that is created by replacing m(Si–N) bonds with m(Al–N) bonds is countered by the incorporation of metal cations into the interstices of α′-Sialon unit cell [1,2]. α′-Sialon ceramics are generally considered to occur in an equiaxed grain morphology and possesses some good properties, such as high hardness, good oxidation and thermal shock resistance [2,3]. α′-Sialon ceramics with elongated grains can be prepared through changing compositions and processing conditions according to the recent study. Their study showed a significant increase in fracture toughness and hardness with the proportion of the elongated α′-Sialon grains in the materials [4–6]. At present, the general synthesis methods of α′-Sialon mainly include reaction sintering, self-propagating high-temperature synthesis and CRN method. CRN method can be used to synthesize low cost but high-quality α′-Sialon powders by using pure SiO_2 and Al_2O_3 as main raw materials [7], and also by using low-cost natural materials [8,9] or industrial waste slag [10,11]. There have been only a few works on synthesizing α′-Sialon powders using blast furnace slag so far. However, there is no report in any literature about synthesis of (Ca,Mg)α′-Sialon powders using titania-bearing blast furnace slag. Therefore, in this work the study on synthesizing (Ca,Mg)α′--Sialon powders using titania-bearing blast furnace slag as a starting material by CRN was carried out. The effects of initial compositions, synthesis temperature and holding time on the

* Corresponding author. Tel.: +86 24 83687719; fax: +86 24 23891072.
E-mail address: jtyz@163.com (T. Jiang).

0272-8842/$34.00
doi:10.1016/j.ceramint.2007.07.005

Table 1
Chemical compositions of the starting materials (mass fraction)

Compound	Titania-bearing BF slag	Silica fume	Bauxite chalmette
SiO_2	24.01	82.91	13.28
Al_2O_3	13.49	0.41	79.30
CaO	27.19	<0.74	<0.35
MgO	7.47	2.92	<0.04
K_2O			0.21
Na_2O	23.16	1.13	<0.20
TiO_2	2.64	8.29	3.07
Fe_2O_3		96.40	2.97
Burning loss	97.49		
Total			99.42

reaction were mainly studied, and synthesis mechanism was discussed.

2. Experimental procedures

Titania-bearing blast furnace slag (Pansteel, China), silica fume (Ferro-alloy factory of Mongolia, China) and bauxite chamote (Yangquan of Shanxi Province, China) were used as starting materials. Table 1 listed the characteristic of these materials. Carbon black (Fushun Petroleum Company, China) was used as reducing agent that contained 95.44 wt% carbon.

The compositions of all the samples were designed to nominally lie on the two-dimensional α′ plane described by the previously given calcium α′-Sialon formula, which are listed in Table 2. Samples are designated by their m and n values in the previously given α′ plane (where the term CA0603 refers to a design composition with $m = 0.6$, $n = 0.3$, and so on). In all the samples, the m:n ratio is 2:1. Thus, their compositions are nominally located on the tie line between Si_3N_4 and RO:3AlN (R = Ca or Mg) in α′ plane with formula $(Ca,Mg)_xSi_{12-3x}Al_{3x}O_xN_{16-x}$ ($x = 0.3$, 0.6, 1.0, 1.4, 1.8 and 2.0) (Fig. 1). The carbon content in CA0603–CA4020 samples was fixed at the stoichiometric value. The sample C1815 referred to the composition with $x = 1.8$ and the carbon content was fixed at 1.5 times the required stoichiometric value.

The mixtures were placed in a polyurethane pot and ball milled in ethanol for 24 h using agate-milling media. Subsequent to milling, the slurry was dried and mixed again for 4 h. Approximately 1.5 g of powder was then uniaxially pressed into pellets that were 15 mm in diameter. The pellets

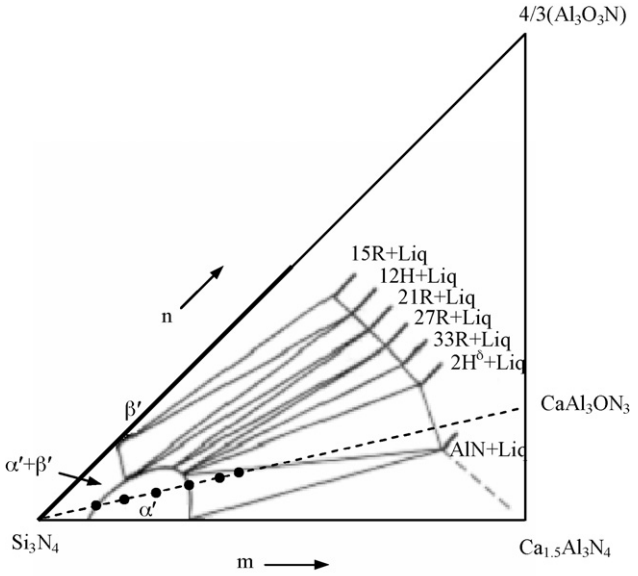

Fig. 1. Phase relationships in α′-Sialon plane by Hewett et al. [12]. The dash line represents the tie line of Si_3N_4–CaO:3AlN and the six dots on the line from left to right indicate the six compositions of $x = 0.3$, 0.6, 1.0, 1.4, 1.8 and 2.0, respectively.

were then pressureless sintered in a $MoSi_2$ electrical furnace in a high-purity nitrogen atmosphere with a flow rate of 0.4 L/min at 1200–1500 °C for 0–14 h. Furnace heating rate was about 5 °C/min, and the cooling rate 4 °C/min. The residual carbon was finally removed by burning the synthesized powder at 580 °C for 6 h in air in order to prevent TiN in the samples from being oxidized.

Each samples was weighed before and after the reaction and the weight loss rate was calculated as follows:

$$\text{weight loss} = \frac{W_i - W_f}{W_i} \times 100 \quad (1)$$

where W_i and W_f are the initial and final weights of the samples before residual carbon removed, respectively.

Phase identification was performed via X-ray diffractometry (XRD, D/MAX-RB) using nickel-filtered Cu Kα radiation. The morphology of samples was characterized via scanning electron microscopy (SEM, SSX-550). An energy dispersive spectrometer (EDS, SSX-550) was used with SEM to chemically analyze specific microstructural features in synthesized powders.

Table 2
Initial compositions of mixtures (mass fraction, %)

Samples	Nominal x	Titania-bearing BF slag	Silica fume	Bauxite chalmette	Carbon black
CA0603	0.3	5.216	65.714	3.659	25.411
CA1206	0.6	10.273	57.178	7.581	24.967
CA2010	1.0	16.783	46.192	12.628	24.396
CA2814	1.4	23.039	35.634	17.480	23.847
CA3618	1.8	29.057	25.478	22.145	23.320
CA4020	2.0	31.980	20.544	24.412	23.064
C1815	1.8	26.023	22.817	19.833	31.327

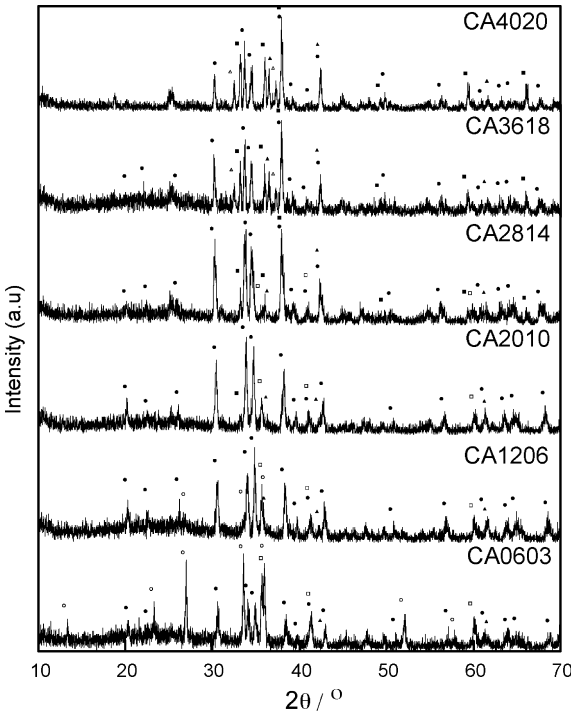

Fig. 2. XRD patterns for the synthesized products at 1500 °C for 6 h in N_2 flow. (●) α′-Sialon; (○) β′-Sialon; (▲) TiN; (■) AlN; (□) SiC; (△) 15R.

3. Results and discussion

3.1. Effect of initial material compositions

The XRD patterns of the synthesized powders with various initial compositions at 1500 °C for 6 h were given in Fig. 2. The results were presented in Fig. 3 based on XRD intensities of two typical peaks of each phase as a function of nominal x values. The reaction products of all the samples consisted mainly of α′-Sialon and TiN (see Fig. 2). But the d value of diffraction peaks of TiN was deviated to the direction of small diffraction angles. It indicated that carbon probably solubilized into TiN cell and result in the expansion of TiN cell, yielding quantitative Ti(N,C) phase. With the compositions shifting towards high x value, β′-Sialon, SiC, AlN, β-$CaSiO_3$ and 15R polytypoid yielded in the products. Moreover, small amount of amorphous phase occurred in the final products.

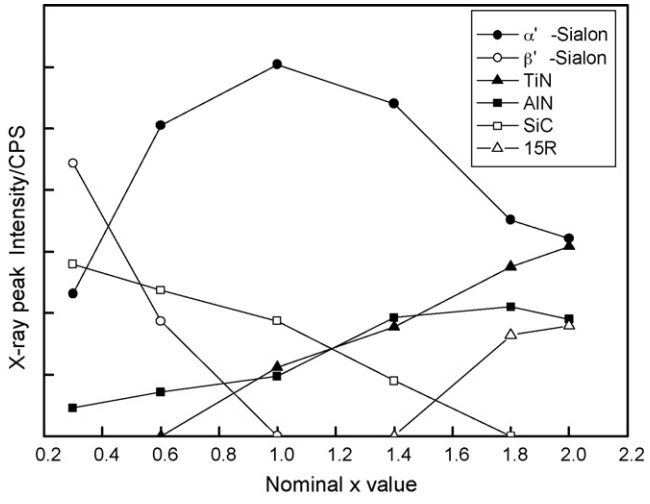

Fig. 3. Phase compositions of reaction products as a function of different x values.

According to the report of Hewett et al. [12] on the phase relationship of Ca–Si–Al–O–N system, in Si_3N_4–AlN:Al_2O_3–Ca_3N_2:3AlN system, i.e. α′-Sialon plane, the composition $x = 0.3$ is located at the lowest limit of the α′ solubility region below which there is a two phases region—α′–β′ (or β-Si_3N_4). Therefore, the appearance of β′-Sialon in the sintered composition ($x = 0.3$) is expected because some of CaO and MgO is exhausted by the formation of the liquid phase and the actual content of Ca^{2+} and Mg^{2+} entering into α′-Sialon is less than 0.3, which have been approved by the present work. According to the XRD patterns of the sample CA0603, the crystalline phases were mainly composed of β′-Sialon, SiC, α′-Sialon and AlN, whereas β′-Sialon became a dominant phase in the sample. With x value increasing, i.e. the composition shifting towards the terminal point Ca(Mg)O:3AlN, β′-Sialon decreased rapidly. β′-Sialon in the sample $x = 0.6$ was not obvious and vanished subsequently, which was different from the conclusion of Komeya et al. [7]. The composition $x = 1.0$ lies in the single-phase region of α′-Sialon where the driving force to form α′-Sialon is maximal, so the amount of α′-Sialon in the products reaches highest value. Subsequently, with the increase of x value, α′-Sialon decreased continuously but the content of TiN and AlN increased, and of SiC decreased gradually until disappear entirely. According to Table 2, with the increase of x value, the addition of titania-bearing blast furnace slag in the starting materials increased so that the content of TiO_2 in the samples increased, therefore the formation of TiN increase as well after the CRN reactions. This showed that the higher x value of the composition was, the higher content of TiN was gained. Simultaneously, when x value was lower, the utilization quantities of blast furnace slag decreased and of silica fume increased, which resulted in the amount of SiC increased in the products. According to the phase relationship of the Ca–Si–Al–O–N system [12], the top limit of Ca–α′-Sialon on the link Si_3N_4–CaO:3AlN is at $x = 1.4$, beyond which there is a multi-phase region—α′-Sialon, liquid phase and AlN polytypoids or AlN. For the compositions between $x = 1.8$ and 2.0, both 15R polytypoid and AlN appeared in the products.

The lattice parameters of (Ca,Mg)α′-Sialon at 1500 °C for 6 h were listed in Table 3. As indicated, with the increase of x value, the solid solubility of Ca^{2+} and Mg^{2+} and the cell dimensions of α′-Sialon increased. When the x value was less than 1.4, the increment of cell dimensions was obvious. More than 1.4, the increment of cell dimensions became sluggish. It has been known that the liquid phase exhausted Ca^{2+} and Mg^{2+} and made the actual content of Ca^{2+} and Mg^{2+} in α′-Sialon grains lower than the nominal compositions. In order to know how much the Ca^{2+} and Mg^{2+} content entered α′-Sialon structure, the present work determined the Ca^{2+} and Mg^{2+} content in α′-Sialon grains by EDS (Table 2). As indicated in

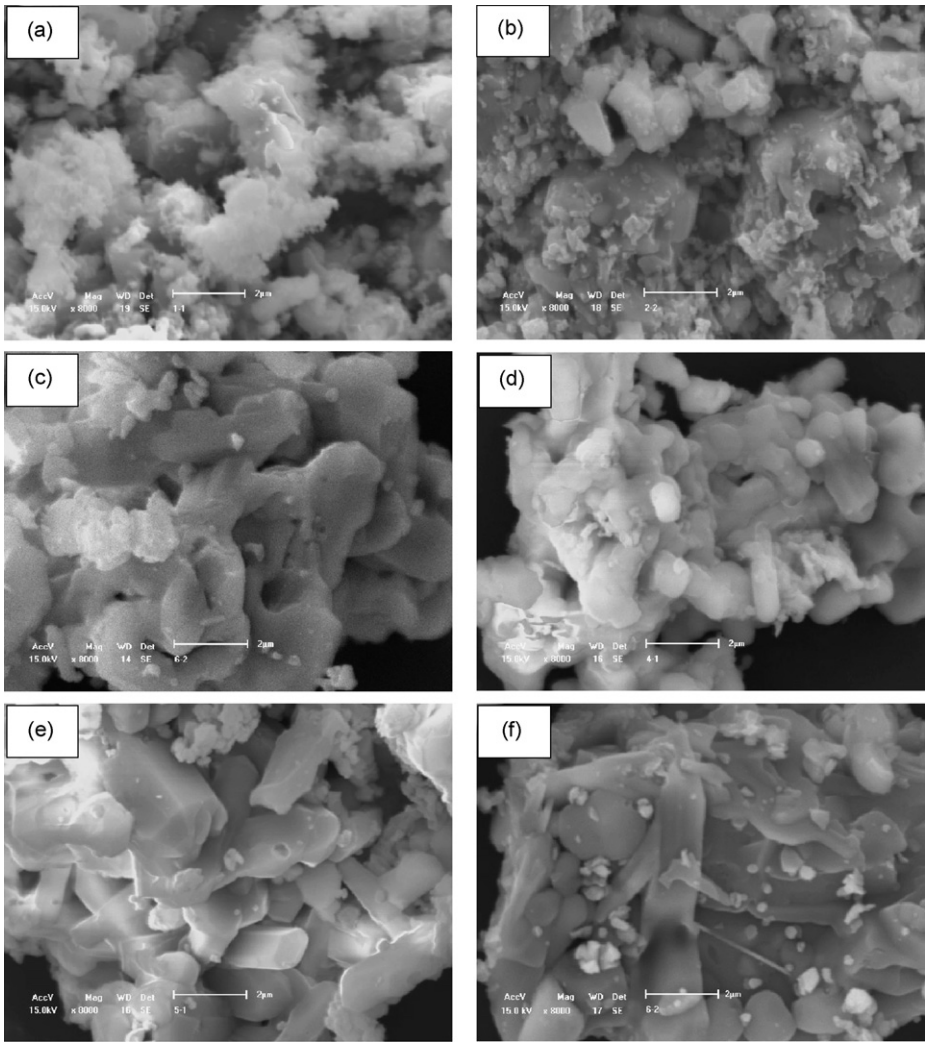

Fig. 4. SEM micrographs of powders synthesized from various initial compositions: (a) $x = 0.3$; (b) $x = 0.6$; (c) $x = 1.0$; (d) $x = 1.4$; (e) $x = 1.8$; (f) $x = 2.0$.

Table 3, most of Ca^{2+} were incorporated into α′-Sialon and the residual remained in the glassy phase. It was noticeable that the amount of Ca^{2+} was much higher than Mg^{2+} in α′-Sialon structure, implying Ca^{2+} being incorporated into α′-Sialon structure was much easier than Mg^{2+}.

The morphology of synthesized powders from various initial composition range of $x = 0.3$–2.0 were observed (see Fig. 4). As indicated in Fig. 4, when the x value was below 1.0, more α′-Sialon grains exhibited equiaxed microstructure. With the compositions shifting to high x value, the amounts of elongated α′-Sialon grains increased obviously, and crystal facets for α′-Sialon were observable. Furthermore, other α′-Sialon grains exhibited longer flake, which was possibly caused by the grains developing incompletely. For many years, the morphology of α′-Sialon grains has been considered as equiaxed. However, the new results [4,6,12,13] indicated that α′-Sialon could also develop into elongated morphology under suitable conditions. Wang et al. [13] first observed the preferred orientation of α′-Sialon grains in hot-pressing samples. Recently Hewett et al. [12], Wood et al. [4] and Wang et al. [6] also reported the increase of elongated Ca–α′-Sialon grains as more Ca^{2+} entered α′-Sialon structure, and considered elongated grains in Ca–α′-Sialon system is easier to occur than in other metal cation-doped α′-Sialon system. According to Shen et al. [14], in the Ln–Si–Al–O–N system, large amounts of liquid phases with low viscosity promoted the formation of elongated α′-Sialon grains, and it was a possible reason of the formation of elongated (Ca,Mg)α′-Sialon in the present work as well. The elongated α′-Sialon grains in synthesized powders could

Table 3
Lattice parameters of (Ca,Mg)α′-Sialon with nominal and determined x values by EDS

Sample	Nominal	Determined		a (Å)	c (Å)	V (Å^3)
	x	x	n(Ca):n(Mg)			
CA0603	0.3	0.18	0.16:0.02	7.847(5)	5.687(6)	303.33
CA1206	0.6	0.32	0.29:0.03	7.858(5)	5.703(3)	305.03
CA2010	1.0	0.86	0.83:0.03	7.884(8)	5.736(4)	308.85
CA2814	1.4	1.12	1.08:0.04	7.900(1)	5.763(6)	311.52
CA3618	1.8	1.50	1.45:0.05	7.942(5)	5.764(2)	314.90
CA4020	2.0	–	–	7.946(8)	5.764(5)	315.27

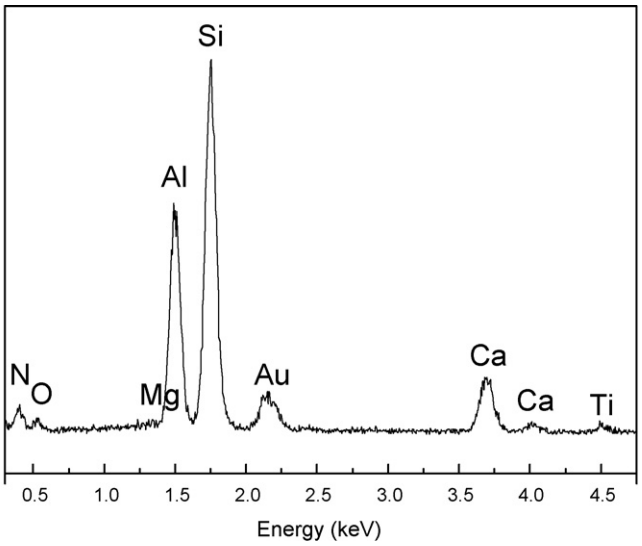

Fig. 5. EDS spectrum of the elongated α′-Sialon grains in synthesized powders.

reinforce the toughness to (Ca,Mg)α′-Sialon ceramics sintered subsequently. In Fig. 4, AlN grains appeared short rods, little beads or irregular morphology, and some thin nanosize grains that are assumed to be TiN grains were observed as well.

Fig. 5 showed the EDS spectrum of the elongated α′-Sialon grains in synthesized powders. As shown in Fig. 5, both Ca^{2+} and Mg^{2+} were incorporated into α′-Sialon structure, and the distribution of Si, Al, O and N was corresponding basically with the content of those in α′-Sialon. Au and Ti in Fig. 5 came from samples metallization and TiN phase, respectively.

3.2. Effect of synthesis temperature on the reaction

The XRD patterns of the sample C1815 in high-purity nitrogen gas with a flow rate of 0.4 L/min at 1200–1500 °C for 8 h were shown in Fig. 6. And the results were plotted in Fig. 7 based on XRD intensities of two typical peaks of each phase as a function of the temperature.

As shown in Figs. 6 and 7, $Al_6Si_2O_{13}$ (Mullite), $MgAl_2O_4$ (Spinel) and $Ca_2Al_2SiO_7$ (Gehlenite) were founded at 1200 °C. It revealed that under the condition the solid phase reactions happened among SiO_2, Al_2O_3, CaO and MgO, and compound oxides were generated, respectively. At the same time, SiO_2 and TiO_2 were reduction-nitridized to form Si_2N_2O and TiN. Besides, small amount of β′-Sialon and 15R polytypoid also appeared in the products. When the synthesis temperature increased to 1250 °C, small amount of α′-Sialon was observed. And contrasting the diffraction standard card of Ca–α′-Sialon ($x = 0.8$), all the diffraction peaks of α′-Sialon formed were deviated to the direction of big diffraction angles. It indicated that the small amount of Ca^{2+} and Mg^{2+} was incorporated into α′-Sialon structure at the moment. Moreover, the CRN reaction of Al_2O_3 happened, yielding AlN. With elevated temperature, the content of $Al_6Si_2O_{13}$, $MgAl_2O_4$, Si_2N_2O and β′-Sialon decreased continuously and disappeared completely at 1300 °C, but $Ca_2Al_2SiO_7$ decreased rapidly after reaching largest content and vanished finally at 1300 °C. Therefore, the

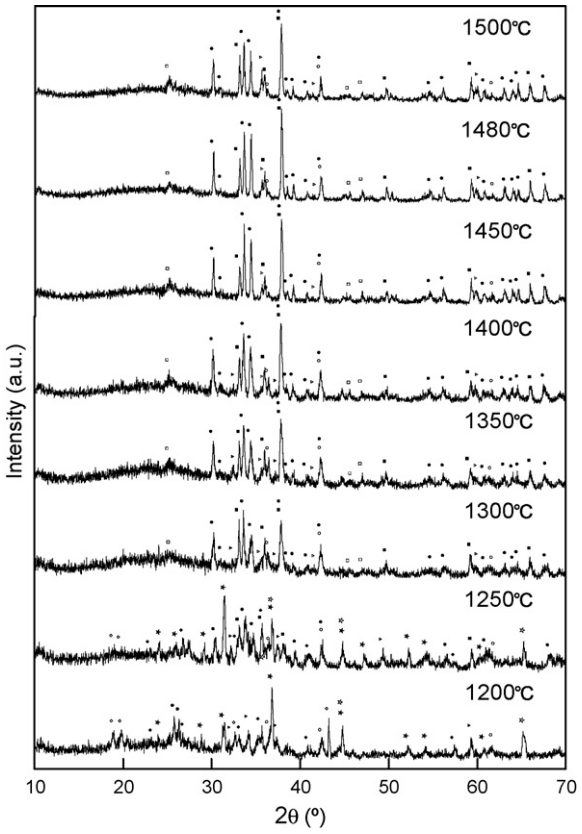

Fig. 6. XRD patterns of the synthesized products fired at various synthesis temperatures for 8 h in N_2 flow: (●) α′-Sialon; (■) AlN; (○) TiN; (△) SiC; (▲) 15R; (◇) Si_2N_2O; (◆) β′-Sialon; (◎) Mullite; (☆) $MgAl_2O_4$; (★) $Ca_2Al_2SiO_7$; (□) β-$CaSiO_3$.

reaction products were mainly composed of α′-Sialon, AlN, TiN, and little SiC, 15R polytypoid and β-$CaSiO_3$ (Wollastonite) at 1300 °C. Thermodynamic analysis indicated that SiC formed only at higher temperature under standard condition. However, the presence of impurity elements such as iron [15,16] altered the phase equilibria by changing the thermodynamic activity, resulting in the formation of liquid phases at lower temperatures and the production of SiC at 1300–1500 °C. Because the starting materials of the present work were composed of natural mineral and metallurgical waste slag containing many impurities, the formation temperature of liquid phases decreased. SiC occurred at such low temperature 1300 °C and increased with increasing temperature. At 1250 °C, the reaction products contained amorphous phases as a result of which the eutectic temperature in the Ca–Mg–Si–Al–O system is 1250 °C [17]. Above this temperature, large amounts of liquid phases would be generated in the reaction system, and the liquid phases were maintained as amorphous phases during decreasing temperature due to the lower reaction temperature.

Above 1350 °C, phase compositions of the products were the same as that of at 1300 °C, however, 15R disappeared completely at 1450 °C. The content of AlN decreased gradually while α′-Sialon increased rapidly, which revealed that AlN participated in the synthesis of α′-Sialon. Above 1400 °C, the

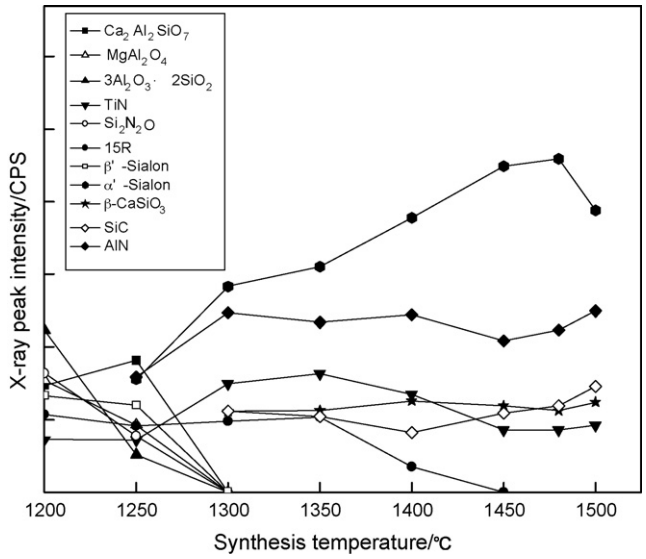

Fig. 7. Phase compositions of reaction products as a function of synthesis temperature.

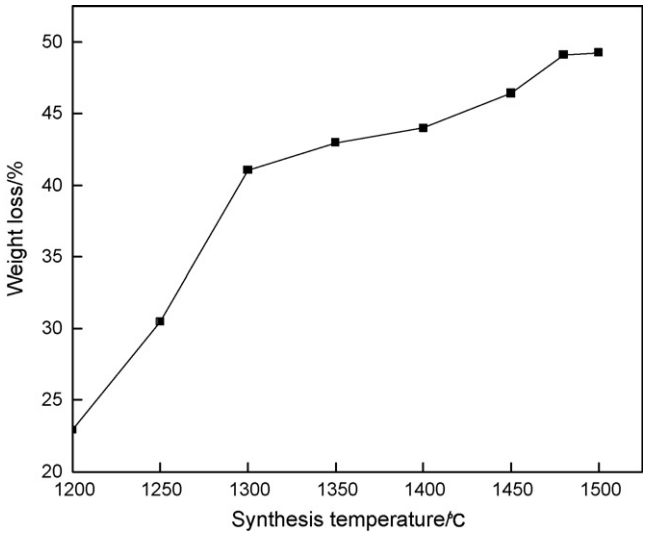

Fig. 8. Variation of the weight loss of reaction products with synthesis temperature.

CRN reactions proceeded sufficiently and hence small amounts of amorphous phases were remained. When the temperature exceeded 1480 °C, the content of α′-Sialon decreased gradually. In contrast, AlN phases increased at the same time. It seemed that α′-Sialon decomposed at this temperature. This indicated that the temperature affected phase compositions of the products significantly. It was necessary that elevating temperature could accelerate the CRN reaction and improve the formation of α′-Sialon, whereas the opposite effect was observed for α′-Sialon if the temperature was more higher while SiC increased simultaneously. By 1480 °C, the whole reactions proceeded thoroughly and the content of α′-Sialon in the products reached the maximum. Consequently, the optimum synthesis temperature was 1480 °C.

The weight loss of the samples as a function of synthesis temperature was shown in Fig. 8. As shown in Fig. 8, the weight loss of the sintered samples was enhanced with the increase of synthesis temperature. The weight loss of the samples exceeded the theoretical value (49.0%) above 1480 °C, whereas the weight loss was also about 23.1% at 1200 °C although larger amount of oxides in the starting materials were not reduction-nitridized. Unexpected weight loss during the reaction was mainly generated by reaction (2) occurred at about 1300 °C and part of SiO was removed with flowing nitrogen, which was approved by the experiment results of many researchers for SiO_2–C–N_2 system. The influencing factors resulting in the volatilization of SiO included N_2 flow rate, synthesis temperature, holding time, etc. [18]. The reaction (2) rate and gas flow rate increased with the increase of synthesis temperature, therefore SiO removed with flowing nitrogen enhanced, which led to higher weight loss of the samples. By 1480 °C, the reactions proceeded sufficiently and loss of SiO decreased obviously, thereby the increase of the weight loss of the samples became slower.

$$SiO_2 + C \rightarrow SiO + CO \quad (2)$$

3.3. Effect of holding time on the reaction

Phase compositions of the sample C1815 as a function of holding time at 1480 °C were presented in Fig. 9 based on XRD intensities of two typical peaks of each phase. As seen in Fig. 9, phase compositions of the products in different holding time were basically similar, which were mainly composed of α′-Sialon, AlN, TiN and small amount of SiC and β-$CaSiO_3$, and all of which were only different in the content. The phase compositions in the products included AlN, SiC, α′-Sialon and TiN, of which AlN became the dominant phase in the sample at 1480 °C for 0 h. This showed that during increasing temperature, most Al_2O_3 and TiO_2 in the starting materials had been reduction-nitridized to AlN and TiN, respectively with the CRN process. It indicated that both of the two CRN

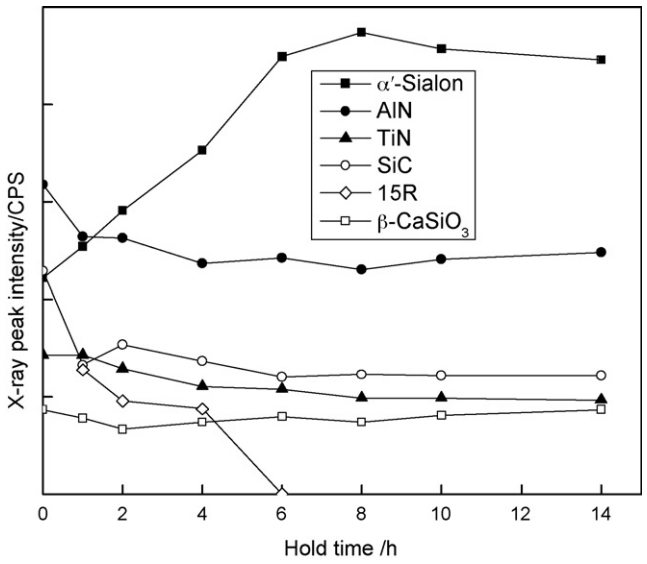

Fig. 9. Phase compositions of reaction products as a function of holding time at 1480 °C.

reactions temperature were lower, which had been approved by the former results as well. Because of no holding temperature, the whole CRN process proceeded insufficiently, which could be confirmed by the more amorphous phases existing in the final products.

Prolonging holding time, the content of α′-Sialon increase and the content of Ca^{2+} and Mg^{2+} being incorporated into α′-Sialon structure increased as well. The content of α′-Sialon reached the maximum after 8 h and then decreased slightly, whereas the opposite effect was observed for AlN. The content of SiC reached the maximum after 2 h and then decreased with α′-Sialon increasing. 15R polytypoid occurred after 1 h and decreased continuously with the increase of holding time, and vanished entirely after 6 h. This showed that 15R polytypoid appeared at the early stage of holding temperature, then decomposed to AlN [19], which could be confirmed from that the content of AlN increased slightly while 15R decreased rapidly in Fig. 9. During holding time small amount of TiN always existed in the samples, but its content hardly changed, which indicated that before holding temperature TiO_2 had been reduction-nitridized to TiN thoroughly. Consequently, at 1480 °C the influence of holding time to phase compositions was not significant, however with holding time increasing, the CRN reactions proceed more sufficiently. The optimum holding time was 8 h for the formation of α′-Sialon in the products, of which the content of α′-Sialon was maximum.

The weight loss of reaction products as a function of holding time was shown in Fig. 10. At 1480 °C for 0 h, the weight loss of the samples reached 43.1% that approached the theoretical value of 49.0%. With the increase of holding time, the weight loss of the samples enhanced and after 8 h reached 49.4% that was much higher than the theoretical value. Meantime, α′-Sialon reached a maximum. The extra weight loss of the samples was mainly resulted in reaction (2). The reaction products included less amount of α′-Sialon at 1480 °C for 0 h, which indicated nitridation reactions occur at present, but only small amount of SiO was nitridized and the residual was removed from the system together with CO following N_2 flow. With the increase of holding time, the loss of CO and SiO removed from the system decreased. Therefore, the relationship of weight loss of the samples as a function of holding time represented that the weight loss increased faster in the early stage of the reactions and decreased gradually with the increase of holding time. The weight loss of the products was less than the theoretical value before 8 h because of incomplete CRN reactions and the formation of SiC that decreased loss of SiO.

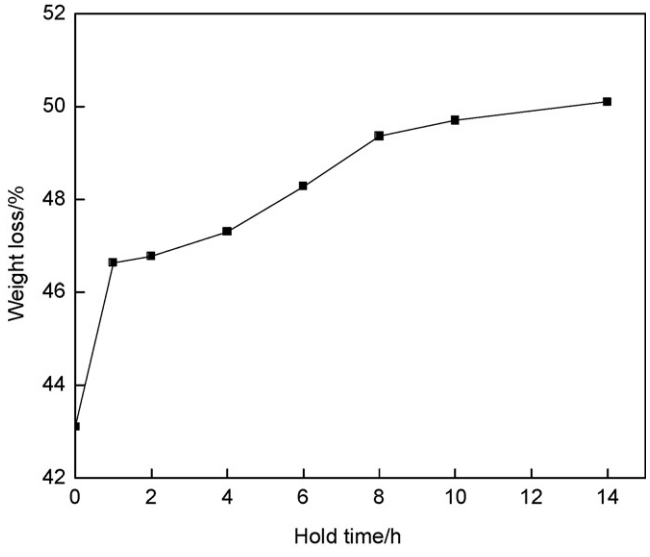

Fig. 10. Variation of the weight loss of reaction products with holding time.

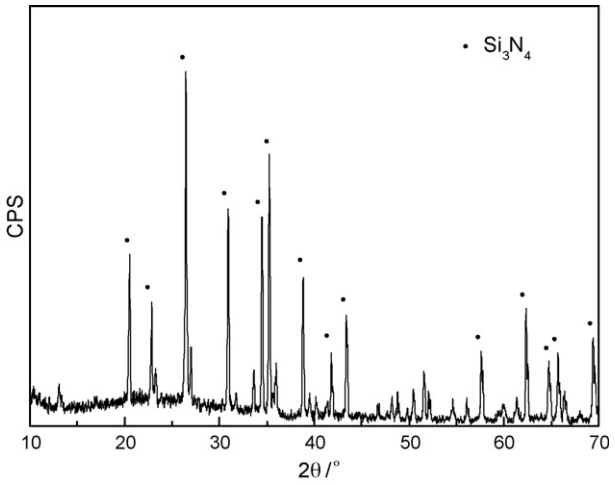

Fig. 11. XRD pattern of white fur-like deposits formed on the wall of crucible and furnace tube.

White fur-like deposits on the wall of crucible and furnace tube were founded after the reaction. Sopicka et al. [18] and Cho et al. [20] also observed the fur-like deposits in their experiments. The XRD analysis confirmed these deposits are α-Si_3N_4 whiskers (see Fig. 11). α-Si_3N_4 whiskers were usually generated via gas phase reaction (3). It indicated further that a mass of SiO, an intermediate phase, was formed in the reaction system during the CRN reactions.

$$3SiO + 3C + 2N_2 \rightarrow Si_3N_4 + 3CO \quad (3)$$

3.4. Discussion of the synthesis mechanism

The reactions among SiO_2, Al_2O_3, CaO and MgO in the initial compositions started at 1200 °C, yielding Mullite, Gehlenite and Spinel. And then Mullite converted to β′-Sialon and 15R polytypoid via the CRN reactions. At the same time, some SiO_2 reacted with both C and N_2 to yield Si_2N_2O, and most of TiO_2 converted to TiN. The following is the main reactions in this stage:

$$2SiO_2 + 3Al_2O_3 \rightarrow 3Al_2O_3{\cdot}2SiO_2 \quad (4)$$

$$SiO_2 + Al_2O_3 + 2CaO \rightarrow Ca_2Al_2SiO_7 \quad (5)$$

$$MgO + Al_2O_3 \rightarrow MgAl_2O_4 \quad (6)$$

$$2SiO_2 + 3C + N_2 \rightarrow Si_2N_2O + 3CO \quad (7)$$

$$3Al_2O_3{\cdot}2SiO_2 + C + N_2 \rightarrow \beta'\text{-Sialon} + 15R\,\text{polytypoid} + CO \quad (8)$$

$$2TiO_2 + 4C + N_2 \rightarrow 2TiN + 4CO \quad (9)$$

Above 1250 °C, reaction (5) and (8) kept on proceeding causing Gehlenite increased and Mullite decreased in the products, where reaction (2) started as well, and SiO_2, Al_2O_3, CaO and MgO in the starting compositions took place the eutectic reaction to form $(Ca,Mg,Si,Al)_xO_y$ liquid phase. CRN of Al_2O_3 started in the stage, yielding AlN. Subsequently, Si_2N_2O, AlN and liquid phase converted to α′-Sialon and β′-Sialon via the reaction with SiO, C and N_2. Then β′-Sialon, AlN and liquid phase were reduction-nitridized further to α′-Sialon. The conclusion was approved by the fact that the content of β′-Sialon in Fig. 6 was basically stable in this stage. Besides reaction (2), the other reactions during the synthesis process are present as follows:

$$2SiO_2 + 3Al_2O_3 + CaO + MgO \rightarrow (Ca, Mg, Si, Al)_xO_y\text{liquid} \quad (10)$$

$$Al_2O_3 + 3C + N_2 \rightarrow 2AlN + 3CO \quad (11)$$

$$Si_2N_2O + AlN + SiO + (Ca, Mg, Si, Al)_xO_y\text{liquid} + C + N_2 \rightarrow (Ca, Mg)\alpha'\text{-Sialon} + \beta'\text{-Sialon} + CO \quad (12)$$

$$\beta'\text{-Sialon} + AlN + SiO + (Ca, Mg, Si, Al)_xO_y\text{liquid} + C + N_2 \rightarrow (Ca, Mg)\alpha'\text{-Sialon} + CO \quad (13)$$

With the increase of temperature, $Al_6Si_2O_{13}$, $MgAl_2O_4$, $Ca_2Al_2SiO_7$, Si_2N_2O and β′-Sialon as intermediate phases converted further to α′-Sialon and AlN, where SiO_2 reacted with C to generate SiC. Small amount of unreacted SiO_2 formed β-$CaSiO_3$ via the reaction with CaO. Above 1480 °C, α′-Sialon decreased slightly and 15R disappeared completely in the products. It was possible that 15R and fractional α′-Sialon decomposed at higher temperature. The main reactions in this stage are given as following:

$$SiO_2 + C \rightarrow SiC + CO \quad (14)$$

$$SiO_2 + CaO \rightarrow \beta\text{-}CaSiO_3 \quad (15)$$

$$15R\,\text{polytypoid} + \alpha'\text{-Sialon} + C \rightarrow AlN + CaO + MgO + SiO + CO \quad (16)$$

4. Conclusions

The synthesis of (Ca,Mg)α′-Sialon powders using titania-bearing blast furnace slag as a starting material by CRN was greatly affected by the starting compositions and process conditions. With the compositions shifting towards high x value, the content of α′-Sialon, TiN and AlN, the solid solubility of Ca^{2+} and Mg^{2+}, the unit cell parameters of α′-Sialon and the amount of elongated α′ grains increased, while β′-Sialon and SiC decreased.

The formation of α′-Sialon in the products increased with elevated temperature. The CRN reactions proceeded more sufficiently with the increasing holding time. The optimum process conditions for the synthesis of α′-Sialon were 1480 °C for 8 h, under which the crystalline phases of the products also included AlN, TiN and small amount of SiC and β-$CaSiO_3$. The volatilization of SiO, an intermediate phase, resulted in a weight loss of the samples, which was enhanced with the increase of synthesis temperature, holding time and N_2 flow rate.

The synthesis mechanism was that SiO_2, Al_2O_3, CaO and MgO in the starting materials reacted mutually to generate Mullite, Gehlenite and Spinel firstly, and then Mullite reacted with both C and N_2 to form β′-Sialon and 15R polytypoid. Simultaneously, SiO_2 and TiO_2 reacted with C and N_2, respectively to yield Si_2N_2O and TiN. Subsequently, AlN generated via CRN of Al_2O_3 reacted with Si_2N_2O, β′-Sialon and $(Ca,Mg,Si,Al)_xO_y$ liquid phase to form α′-Sialon. Small amount of unreacted SiO_2 reacted with CaO to form β-$CaSiO_3$. After 8 h at 1480 °C, 15R and some α′-Sialon decomposed.

Acknowledgement

The work was supported by the National Natural Science Foundation of China under grant no. 50034010.

References

[1] S. Hampshire, H.K. Park, D.P. Thompson, et al., α′-Sialon ceramics, Nature 274 (1978) 880–882.
[2] T. Ekström, M. Nygren, Sialon ceramics, J. Am. Ceram. Soc. 75 (2) (1992) 259–276.
[3] G.Z. Cao, M. Metselaar, α′-Sialon ceramics: a review, Chem. Mater. 3 (1991) 242–252.
[4] C.A. Wood, H. Zhao, Y.B. Cheng, Microstructural development of Ca α-Sialon ceramics with elongated grains, J. Am. Ceram. Soc. 82 (2) (1999) 421–428.
[5] I.W. Chen, A. Rosenflanz, A tough Sialon ceramic based on α-Si_3N_4 with a whisker-like microstructure, Nature 389 (1997) 701–704.
[6] P.L. Wang, C. Zhang, W.Y. Sun, et al., Characteristics of Ca–α-Sialon—phase formation, microstructure and mechanical properties, J. Eur. Ceram. Soc. 19 (1999) 553–560.
[7] K. Komeya, C. Zhang, M. Hotta, et al., Hollow beads composed of nanosize Ca α-Sialon grains, J. Am. Ceram. Soc. 83 (4) (2000) 995–997.
[8] C. Zhang, K. Komeya, J. Tatami, et al., Synthesis of Mg–α′-Sialon powders from talc and halloysite clay minerals, J. Eur. Ceram. Soc. 20 (2000) 1809–1814.
[9] J.W.T. Van Rutten, R.A. Terpstra, J.C.T. Van der Heijde, et al., Carbothermal preparation and characterization of Ca–α′-Sialon, J. Eur. Ceram. Soc. 15 (1995) 599–604.
[10] K.M. Liu, F.M. Wang, W.C. Li, et al., Synthesis of Ca–α′-Sialon–SiC powders from blast furnace slag and optimization of its synthesis, J. Univer. Sci. Technol. Beijing 23 (5) (2001) 404–408.
[11] W.W. Chen, P.L. Wang, D.Y. Chen, et al., Synthesis of (Ca,Mg)α′-Sialon from slag by self-propagation high-temperature synthesis, J. Mater. Chem. 12 (2002) 1199–1202.
[12] C.L. Hewett, Y.B. Cheng, B.C. Muddle, Phase relationships and related microstructural observations in the Ca–Si–Al–O–N system, J. Am. Ceram. Soc. 81 (7) (1998) 1781–1788.
[13] H. Wang, Y.B. Cheng, B.C. Muddle, et al., Preferred orientation in hot-pressed Ca α-Sialon ceramics, J. Mater. Sci. Lett. 15 (16) (1996) 1447–1449.
[14] Z.J. Shen, L.O. Nordberg, M. Nygren, et al., α-Sialon grains with high aspect ratio—utopia or reality? in: Engineering Ceramics '96. Higher Reliability through Processing, Kluwer Academic Pubilshers, Netherlands, 1997, pp. 169-178.
[15] G. Lee, I.B. Cutler, Sinterable sialon powder by reaction of clay with carbon and nitrogen, Am. Ceram. Soc. Bull. 58 (1979) 869–871.

[16] S.A. Siddqi, A. Hendry, The influence of iron on the preparation of silicon nitride form silica, J. Mater. Sci. 20 (1985) 3230–3238.
[17] C.R. Robbins, H.F. McMurdie, E.M. Levin, Phase Diagrams for Ceramists, Am. Ceram. Soc., Columbus, OH, 1964.
[18] L.M. Sopicka, R.A. Terpstra, R. Metselaar, Carbothermal production of β′-Sialon from alumina, silica and carbon mixture, J. Mater. Sci. 30 (1995) 6363–6369.
[19] J.Y. Qiu, J. Tatami, C. Zhang, et al., Influence of starting material composition and carbon content on the preparation of Mg–α′-Sialon powders by carbothermal reduction–nitridation, J. Eur. Ceram. Soc. 22 (2002) 2989–2996.
[20] Y.W. Cho, J.A. Charles, Synthesis of nitrogen ceramic powders by carbothermal reduction and nitridation. Part 2. Silicon aluminium oxynitride (Sialon), Mater. Sci. Technol. 7 (5) (1991) 399–406.